Numerical Analysis of Micro-Structural Characterization of (TiB+TiC0/Ti6Al4V Material"

Krishna Bhushan Patel[1], Prof. Vivek Babele[2]
[1, 2] Dept of mechanical engineering
[1, 2] RGPM, Bhopal

Abstract- *In the development of Titanium alloys and composite materials, the addition of boron and carbide has emerged as an efficient way to provide vital enhancements to special properties including strength, stiffness, and wear resistance. Innovations created with (TiB+TiC)/Ti6Al4V materials to the current purpose have resulted from typical metallurgic techniques that are equally accustomed produce alternative metal alloys and composites. The (TiB+TiC)/Ti6Al4V reinforcement innovate boron-carbide modified titanium, however, is exclusive in that it forms in situ during processing. Additionally, (TiB+TiC)/Ti6Al4V materials are shaped employing a wide range of process strategies and conditions, and with a spread of initial constituent materials. The complexity of the microstructures of (TiB+TiC)/Ti6Al4V materials, along with the variety of process schemes and the in situ formation of (TiB+TiC)/Ti6Al4V, mean that ancient analysis and development strategies are insufficient for complete and correct application of those alloys and composites. The viability of various process strategies are verified, and therefore the mechanical properties of the many of those (TiB+TiC)/Ti6Al4V materials are studied, however an in-depth understanding of the relationships between the microstructure, processing, and resultant properties has needed more investigation. to design a (TiB+TiC)/Ti6Al4V material with a desired set of properties, it's essential to understand however the process strategies affect the microstructure, and the way the microstructure affects the properties of interest. This can be particularly of relevance for (TiB+TiC)/Ti6Al4V materials because sufficient process flexibility exists for the generation of a wide range of various microstructures.*

The focus of this analysis has been to research the microstructures of (TiB+TiC)/Ti6Al4V materials, and verify the relationships between the microstructure, process strategies, and resultant properties. It's hoped that this work can result in more economical materials design of (TiB+TiC)/Ti6Al4V modified alloys and composites. More specifically, analysis objectives included:

1. *Unbiased quantitative characterization and illustration of the microstructures of (TiB+TiC)/Ti6Al4V materials utilizing typical and recently developed stereological strategies on two-dimensional (2D) examples.*
2. *Creation of digital three-dimensional (3D) microstructures of (TiB+TiC)/Ti6Al4V materials using serial sectioning techniques.*
3. *Decisive the relationships between the process strategies of those materials and the critical aspects of the microstructures with regard to the resultant mechanical properties of interest.*
4. *Developing the inspiration for the strategies to be developed for the simulation of real microstructures and the creation of virtual microstructures to be used in materials design of (TiB+TiC)/Ti6Al4V modified alloys and composites.*

The results of this work have provided the groundwork for a contemporary and economical materials style methodology combining ancient metallurgic techniques with computer simulations, a huge improvement over what has traditionally been a haphazard, trial-and-error materials development approach. Additionally, data gained and a couple of discoveries created during this analysis can facilitate with the implementation of (TiB+TiC)/Ti6Al4V materials in a variety of industrial and industrial applications.

I. INTRODUCTION

The high strength-to-weight ratio and excellent corrosion resistance of titanium began to garner interest in the metal soon after World War II, following the invention and development of the commercial Kroll production process. However, the poor wear resistance and relatively low modulus of pure titanium and early alloys spawned research into titanium-based modified alloys and metal matrix composite materials (MMCs) to improve the overall mechanical properties. With the development of discontinuously reinforced titanium matrix MMCs (also known as DRTi composites), and modified alloys containing titanium boride whiskers, it has been shown that adding even relatively small additions of boron to conventional titanium alloys can provide significant improvements to important properties, including strength, stiffness, wear resistance, and micro-structural stability.

1.2 Microstructure

Microstructure is the small scale structure of a material, defined as the structure of a prepared surface of material as revealed by a microscope above 25× magnification. The microstructure of a material (such as metals, polymers, ceramics or composites) can strongly influence physical properties such as strength, toughness, ductility, hardness, corrosion resistance, high/low temperature behavior or wear resistance. These properties in turn govern the application of these materials in industrial practice. Microstructure at scales smaller than can be viewed with optical microscopes is often called nanostructure, while the structure in which individual atoms are arranged is known as crystal structure. The nanostructure of biological specimens is referred to as ultrastructure. A microstructure's influence on the mechanical and physical properties of a material is primarily governed by the different defects present or absent of the structure. These defects can take many forms but the primary ones are the pores. Even if those pores play a very important role in the definition of the characteristics of a material, so does its composition. In fact, for many materials, different phases can exist at the same time. These phases have different properties and if managed correctly, can prevent the fracture of the material.

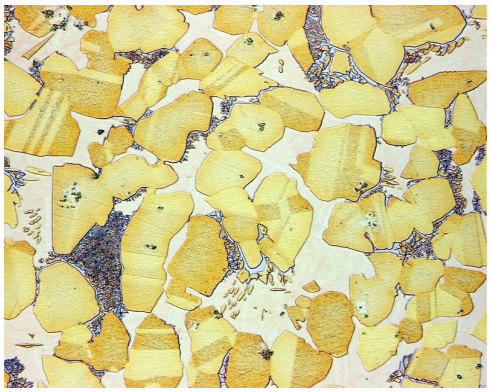

Figure 1.1 Metallography allows the metallurgist to study the microstructure of metals.

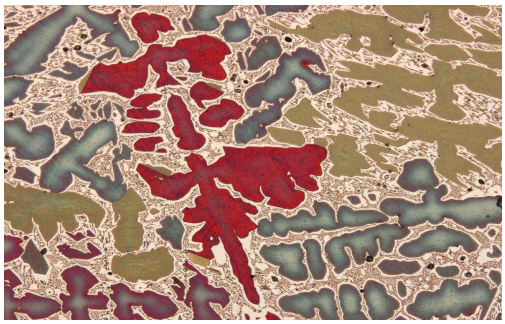

Figure 1.2 a micrograph of bronze revealing a cast dendritic structure

Metallography allow the metallurgist to study the microstructure of metal and a micrograph of bronze revealing a cast dendritic structure shown in the figure 1.1 and figure 1.2 respectively.

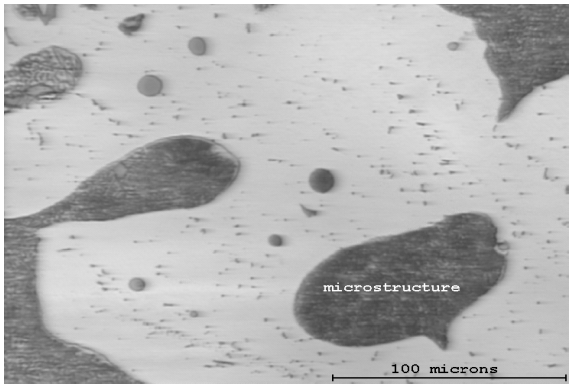

Figure 1.3 Al-Si microstructure

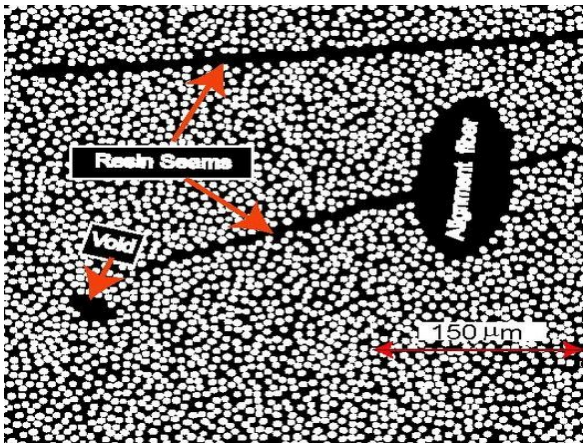

Figure 1.4 a Computer Simulated Microstructure of Composite Material

Figure 1.5 Aluminum copper (4 at% Cu) alloy showing copper precipitation within the aluminum matrix.

Al-Si microstructure and Computer Simulated Microstructure of Composite Material and Aluminum copper (4 at% Cu) alloy showing copper precipitation within the

aluminum matrix shown in the figure 1.3, 1.4, and 1.5 respectively.

1.3 Titanium Alloys and Composites

1.3.1 Titanium Allow

Titanium alloys are metals that contain a mixture of titanium and other chemical elements. Such alloys have very high tensile strength and toughness (even at extreme temperatures). They are light in weight, have extraordinary corrosion resistance and the ability to withstand extreme temperatures. However, the high cost of both raw materials and processing limit their use to military applications, aircraft, spacecraft, medical devices, highly stressed components such as connecting rods on expensive sports cars and some premium sports equipment and consumer electronics.
Although "commercially pure" titanium has acceptable mechanical properties and has been used for orthopedic and dental implants, for most applications titanium is alloyed with small amounts of aluminum and vanadium, typically 6% and 4% respectively, by weight. This mixture has a solid solubility which varies dramatically with temperature, allowing it to undergo precipitation strengthening. This heat treatment process is carried out after the alloy has been worked into its final shape but before it is put to use, allowing much easier fabrication of a high-strength product.

1.3.3 Properties of Titanium Allow

Generally, beta-phase titanium is the more ductile phase and alpha-phase is stronger yet less ductile, due to the larger number of slip planes in the bcc structure of the beta-phase in comparison to the hcp alpha-phase. Alpha-beta-phase titanium has a mechanical property which is in between both.
Titanium dioxide dissolves in the metal at high temperatures, and its formation is very energetic. These two factors mean that all titanium except the most carefully purified has a significant amount of dissolved oxygen, and so may be considered a Ti–O alloy. Oxide precipitates offer some strength (as discussed above), but are not very responsive to heat treatment and can substantially decrease the alloy's toughness.

Many alloys also contain titanium as a minor additive, but since alloys are usually categorized according to which element forms the majority of the material, these are not usually considered to be "titanium alloys" as such. See the sub-article on titanium applications.

Titanium alone is a strong, light metal. It is stronger than common, low-carbon steels, but 45% lighter. It is also twice as strong as weak aluminum alloys but only 60% heavier. Titanium has outstanding corrosion resistance to sea water, and thus is used in propeller shafts, rigging and other parts of boats that are exposed to sea water. Titanium and its alloys are used in airplanes, missiles and rockets where strength, low weight and resistance to high temperatures are important. Further, since titanium does not react within the human body, it and its alloys are used to create artificial hips, pins for setting bones, and for other biological implants.

1.3.6 TIB (Titanium with Boron Modified)

Titanium di-boride (TiB_2) is an extremely hard ceramic which has excellent heat conductivity, oxidation stability and resistance to mechanical erosion. TiB_2 is also a reasonable electrical conductor, so it can be used as a cathode material in aluminum smelting and can be shaped by electrical discharge machining.

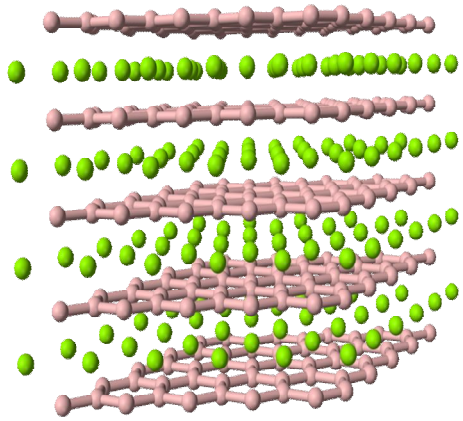

Figure 1.6 Titanium do boride

Physical Property

TiB_2 is very similar to titanium carbide, an important base material for cermets, and many of its properties (e.g. hardness, thermal conductivity, electrical conductivity and oxidation resistance) are superior to those of TiC.

- Exceptional hardness (25–35 GPa Vickers at room temperature, more than three times harder than fully hardened structural steel), which is retained up to high temperature.
- High melting point (3225 °C),
- High thermal conductivity (60-120 W/(m K)),
- High electrical conductivity (~10^5 S/cm)

1.3.7 TIC (Titanium Carbide)

Titanium carbide, TiC, is an extremely hard (Mohs 9–9.5) refractory ceramic material, similar to tungsten carbide. It has the appearance of black powder with the sodium chloride (face-centered cubic) crystal structure. As found in nature its crystals range in size from 0.1 to 0.3mm.

Titanium carbide is used in preparation of cermet, which are frequently used to machine steel materials at high cutting speed. It is also used as an abrasion-resistant surface coating on metal parts, such as tool bits and watch mechanisms. Titanium carbide is also used as a heat shield coating for atmospheric reentry of spacecraft.

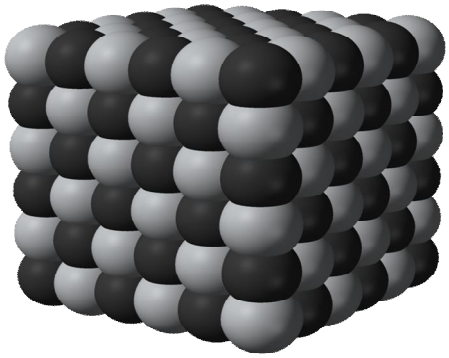

Figure 1.7 Titanium Carbide

1.7 Processing of Metal Matrix Composites

In general the most common manufacturing MMC technologies are divided primarily into two main parts: primary and the secondary. The primary processing is the composite production by combining ingredient materials (powdered metal and loose ceramic particles, or molten metal and fiber performs), but not necessarily to final shape or final microstructure and the secondary processing is the step which obviously follows primary processing, and its aim is to alter the shape and microstructure of the material (shape casting, forging, extrusion, heat treatment, machining). Secondary processing can change the constituents (phase, shape) of the composite. So, MMCs can be made by different ways.

Powder Metallurgy

The powder metallurgy is one of the popular solid state methods used in production of metal matrix composites. Powder processing methods in conjunction with deformation processing are used to fabricate particulate or short fiber reinforced composites. This typically involves cold pressing and sintering, or hot pressing to fabricate primarily particle or whisker reinforced MMCs [12]. The matrix and the reinforcement powders are blended to produce a homogeneous distribution; it is usually used for high melting point matrices and avoids segregation effects and brittle reaction product formation prone to occur in liquid state processes. This method permits to obtain discontinuously particle reinforced AMCs with the highest mechanical properties. These AMCs are used for military applications but remain limited for large scale production.

Powder metallurgy process is mainly consists of three phases. The first phase gives the preparation of the powder that is the constituents of the mixture and it follows the successive stages, In the second phase the powder products are mixed together with the reinforcement , The third process is the process of consolidation, during which the powders of worked mixture are welded together by sintering to form final product. Ceramics or other particles and then compacted in the desired forms.

Diffusion Bonding

Diffusion bonding is a common solid-state processing technique for joining similar or dissimilar metals. Inter diffusion of atoms between clean metallic surfaces, in contact at an elevated temperature, leads to bonding. The principal advantages of this technique are the ability to process a wide variety of metal matrices and control of fiber orientation and volume fraction. Among the disadvantages are long processing times, high processing temperatures and pressures (which makes the process expensive), and a limitation on the complexity of shapes that can be produced. There are many variants of the basic diffusion bonding process, although all of them involve simultaneous application of pressure and high temperature.

II. STIR CASTING

The simplest and most commercially used technique is known as ‘vortex technique’ or ‘stir casting technique’ it is attractive because of simplicity, low cost of processing, flexibility, most economical for large sized components to be prepared as well as production of near net shaped components. The vortex technique involves the introduction of pretreated ceramic particles into the vertex of molten alloy created by the rotating impeller. Figure 1.8 shows the stir casting set up.

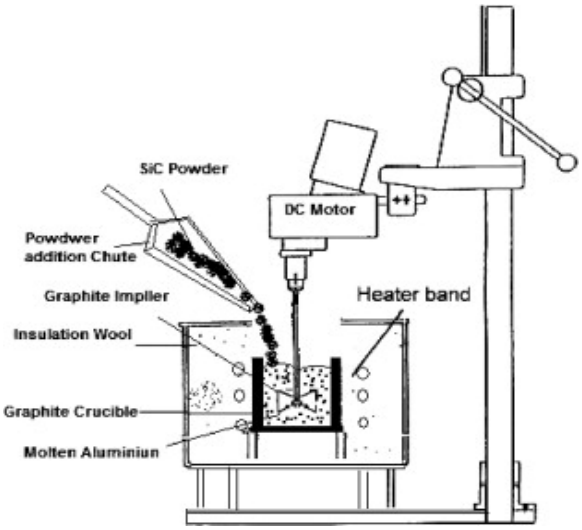

Figure 1.8 Stir casting method

An interesting recent development in stir casting is a two-step mixing process. In this process, the matrix material is heated to above its liquids temperature so that the metal is totally melted. The melt is then cooled down to a temperature between the liquids and solidus points and kept in a semi-solid state. At this stage, the preheated particles are added and mixed. The slurry is again heated to a fully liquid state and mixed thoroughly. This two-step mixing process has been used in the fabrication of aluminum. Among all the well-established metal matrix composite fabrication methods, stir casting is the most economical. For that reason, stir casting is currently the most popular commercial method of producing aluminum based composites [13].

Squeeze Casting: Squeeze casting is also known as liquid metal forging, is a combination of casting and forging process (figure 1.9). The molten metal is poured into the bottom half of the pre-heated die. As the metal starts solidifying, the upper half closes the die and applies pressure during the solidification process.

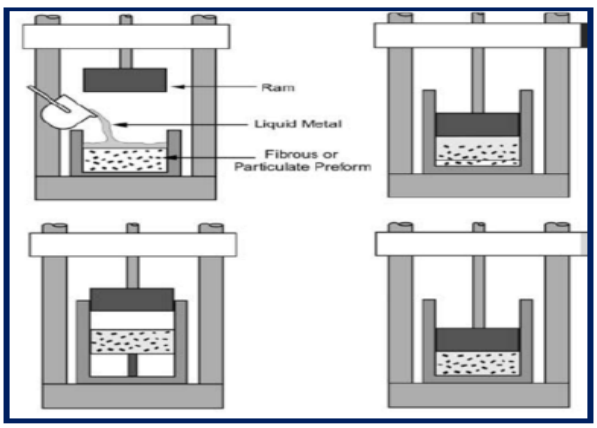

Figure 1.9 Squeeze casting or pressure infiltration process

The amount of pressure thus applied is significantly less than used in forging, and parts of great detail can be produced. Coring can be used with this process to form holes and recesses. The porosity is low and the mechanical properties are improved. Both ferrous and non-ferrous materials can be produced using this method.

Compo-casting

Compo-casting is a liquid state process in which the reinforcement particles are added to a solidifying melt while being vigorously agitated. It has been shown that the primary solid particles already formed in the semi-solid slurry can mechanically entrap the reinforcing particles, prevent their gravity segregation and reduce their agglomeration [14]. These will result in better distribution of the reinforcement particles. The lower porosity observed in the castings has been attributed to the better wettability between the matrix and the reinforcement particles as well as the lower volume shrinkage of the matrix alloy.

III. MODELLING INTRODUCTORY

During the early periods of Extrusion process analysis and die design, researchers depend on extensive experiments which are costly and time consuming. To overcome the above problem and to cut down the analysis time different numerical methods have been proposed to reduce the material cost and dependency on tedious experiments. The application of numerical technique to metal forming problems has been growing rapidly, as a result of significant development attained in computer hardware and software. Among different numerical techniques, finite element method (FEM) has been demonstrated to be the most excellent way for analyzing metal forming problems. Normally, any physical system can be illustrated in the form of partial differential equations utilizing the understanding of mathematical formulations and engineering sciences. In particular, metal forming problems can be mathematically simulated by applying the theory of elasticity and plasticity, solving a set of second order partial differential equations. Finite element has turn out to be the most accepted technique for solving such equations. FEM has been effectively applied to the solution of steady state and transient problems and non-linear situations of one-, two-, and three dimensional geometrical forms and different material behaviors. The finite element discretization process, like the finite difference process, transforms partial differential equations into algebraic equations. The simulation of aluminum extrusion/forging process is carried out by different researchers using different finite element software. A lot of numerical analysis in the past few years suggests that experimental analysis should be

performed to validate the FEM results obtained for different influencing parameters.

In present work we perform the similar FEM approach for titanium matrix composite billets with the help of numerical analysis predict the mechanical properties and validate with the existing experimental results of **Wang et al** and with the help of simulation we can also predict the Variation of punch load with punch travel at different friction factor.

The main objective of this proposed Modelling:

- Draw Fem Simulation 3d model for hot in-direct extrusion
- Validations with experimental data
- Punch load and Punch displacement
- Strength of billet
- FEM with different di angle

3.2 Modelling of the System

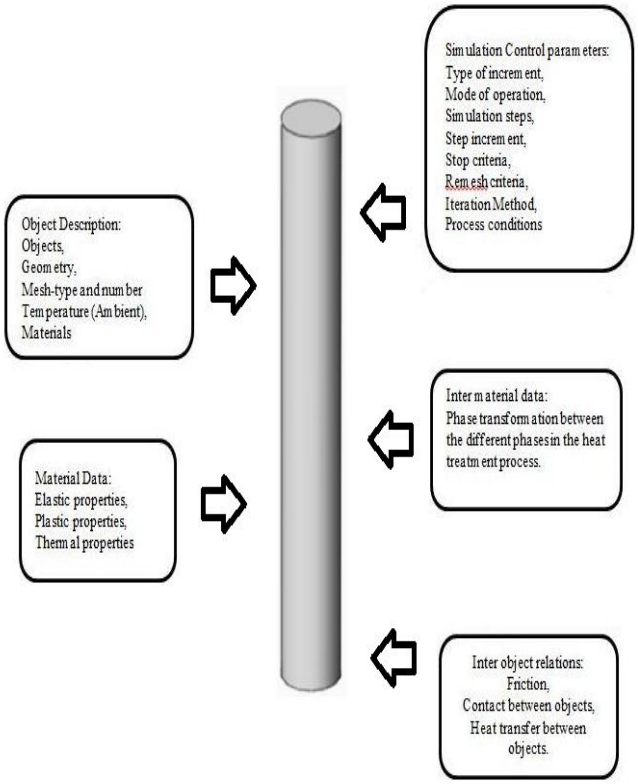

Figure 3.1 Major input parameters for FEM simulation

Figure 3.1 represents the major input parameters which are in application in the present simulation process. The software consists of three key features:

3.2.1 Pre-processor:

The objective of this module is to feed the input data required to perform numerical analysis. The models of deformable work piece and the dies required for the operation are imported.

3.2.2 Simulation

The Finite element analysis performs the simulation according to the given input data.

3.2.3 Post-processor

The data obtained from the simulation analysis is viewed in a graphical user interface. The graphical representation gives us the geometry data such as effective stress, effective strain, temperature, mean stress, total velocity of the product at various sections. In the post processor section the data can be extracted for further comparison and other application obtained from the numerical analysis.

3.3 Simulation control

The SI unit convention with the Langrangian incremental type followed by a deformation mode is selected for the FEM simulation. The mechanical, thermal and phase transformations simulates the deformation into the work piece. Terminate the operation is performed when the specified distance is reached by the primary die and aborting distance are in combination with the reference points. The step size is the crucial for the simulation to perform the operation. The step size can be controlled by two ways either by die displacement or by time increment. The present simulation analysis is performed by controlling the time increment. During the simulation severe plastic deformation takes of the work piece (Slave). This Severe plastic deformation causes the work piece to distort which can be used further (negative Jacobean). The operation to be performing re-meshing after the mesh is distorted. The process of re-meshing is substituting the distorted mesh with a new mesh along with interpolating the field variables (strain, velocity, damage, and temperature, etc.) from old mesh to new mesh. The object re-meshing is performed to a slave (billet). The re-meshing depends on the interference between the primary die and the billet. The depth of interference is the depth an element edge of the slave object crosses the surface of a master object.

3.4 Simulation modelling

In finite element modelling (FEM), combined extrusion-forging and combined extrusion process technique is used to produce different types of collet chuck holders, at varying rate of ram displacements. The Non-linear-equations

are solved with the help of direct iteration method and the Newton-Raphson method. Flow behavior was studied with, a modified Lagrangian method for the finite element code. The initial estimate of the Conjugate Gradient method, the direct iteration method is employed in the solution procedure, which is further used to find the velocity error and force error, obtained as 0.004 and 0.03 respectively. It has assumed that the billet was rigid plastic and the die, container, and flow guide is indeed rigid during the simulation process. The four-noded tetrahedron elements have been employed. In this finite element simulation, an isothermal process was adopted.

3.5 Simulation for the present problem

In the present CEF and CE processes a cylindrical billet made of Ti6Al4V alloy was selected as the matrix alloy, (chemical composition shown in Table 3.1) is forced by the punch, against the bottom die, which is stationary. Followed by extrusions in the various directions and filling in the radial orientation of the die cavity. The axis-symmetry 3d model extrusion die set-up as shown in Figure 3.2.

Table 3.1 Chemical Composition of Different Material

Material	composition					RF	TiB	TiC	Mole Ratio
	AlV	AL	B4C		C	vol %		vol %	vol %
Ti6Al4V	Ti					TiB:TiC			
	7.75	1.89	0.62	0.40	Bal.	5.0	2.6	2.4	1.1

A defined friction factor for the billet, die, container and flow guide interfaces has been set for the hot indirect extrusion condition. The four node tetrahedron elements have employed. A mesh independence test was performed to use ANSYS FEM the analyses to get the desired and accurate punch loads at various frictional conditions friction factor of 0.12, 0.18 and 0.37 which is calibrated at different ranges of elements (at ram velocity of 1.1 mm/min for first product as an illustration). The work piece is modelled using approximately 20000 meshing elements and 3489 nodes for the billet without hampering the accuracy of the final results.

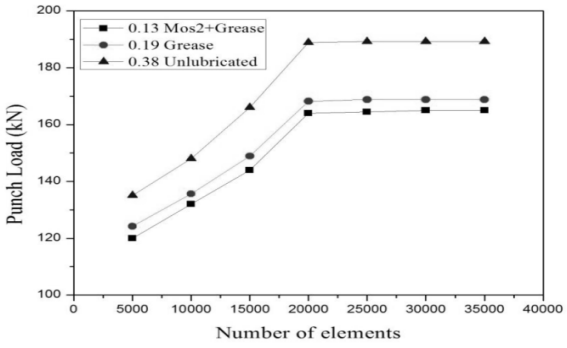

Similar grid independence test were conducted at different ram velocities which has negligible effect. The temperature of all the objects is set to 35ºC. The process parameters assumed for the current analysis is discussed below. The flow stress is obtained from the experimental results during compression test. For the present finite element analysis, isothermal condition is assumed. Direct iteration method and Newton-Raphson methods have been adopted for solving the non-linear equations. A good initial guess has generated for the Newton-Raphson method using the direct iteration method, for the speedy final convergence. When the plastic deformation reaches the steady state, the simulation is stopped.

The assumptions made in the simulation process are as follows:

1. The material of die has taken as rigid
2. Ti6Al4V is taken as the billet in the simulation process and modelled using von Mises yield criterion for an isotropic rigid plastic material.
3. The friction factor for the interface work piece/die is considered as constant, which has found from ring test experimentally.
4. The billet axis has incorporated with the centroid of the die orifice.
5. Global re-meshing criterion and logarithmic interpolation.

For every friction condition three ram velocities are considered, these are:

i. 0.5 mm/min,
ii. 1.1 mm/min, and
iii. 2 mm/min.

IV. RESULTS AND DISCUSSIONS

4.1 Numerical Analysis

The method numerical analysis is carried out to get the final product from the initial cylindrical billet of 82 mm diameter and detail dimensions of the final product obtained is of 76 mm diameter and 50 mm length by compressing the round billet inside a rigid container with required cavity by a rigid punch to demonstrate the process of combined extrusion. The dies and punch plate used for simulation was same as that of experimental sets.

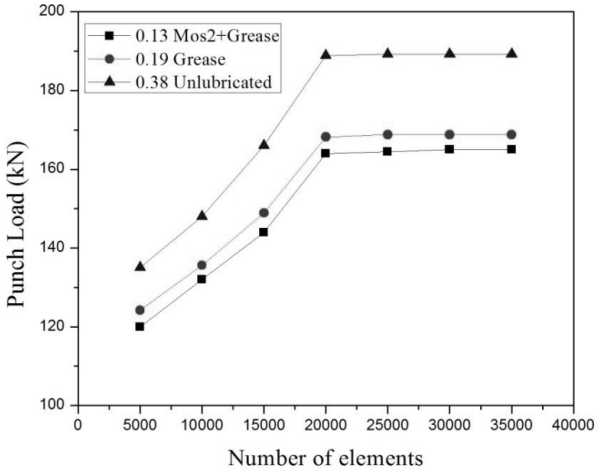

Figure 4.1 Grid independence test result

A defined friction factor for the billet, die, container and flow guide interfaces has been set for the hot indirect extrusion condition. The four node tetrahedron elements have employed. A mesh independence test was performed to use ANSYS FEM the analyses to get the desired and accurate punch loads at various frictional conditions friction factor of 0.12,0.18,0.37 which is calibrated at different ranges of elements (at ram velocity of different mm/min for first product as an illustration in figure 4.1).

4.2 Extrusion Load at different frictions and ram velocities

4.2.1 Variation of punch load with punch travel at friction factor of 0.12, 0.18, 0.37 at 45° Die angle

Figures 4.2 to 4.4 gives comparison of punch load with punch movement for different velocities using lubricant MoS2 + grease (60:40) with friction factor 0.12,0.18,0.37 and Die angle 45° and 100% grease and no lubrication respectively. The maximum extrusion loads at flashing are provided in Table 4.1. The ram displacement behaviors show that the total process can be assumed to consist of four stages:

- Initial stage, the load gradually increases backward extrusion takes place,
- Second stage, forward and lateral extrusion takes place,
- Combined stage, both extrusion and forging takes place for corner filling,
- The unsteady state stage, steep rise in load to form flash. As the metal flow are hindered, redundant work increases, subsequently the load increases unsteadily.

Table No. 4.1 for 45° Die angle

Sl. No.	Friction factor	Ram velocity (mm/min)	Peak load at flashing, kN
1	0.12	0.5	157.70
2		1.0	164.00
3		2.0	172.10
4	0.18	0.5	161.70
5		1.0	168.40
6		2.0	173.70
7	0.37	0.5	174.00
8		1.0	189.50
9		2.0	195.4

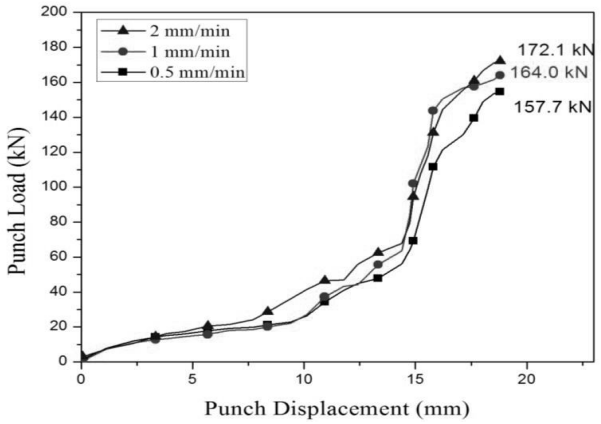

Figure 4.2 Variation of punch load with punch travel at friction factor of 0.12 at 45° Die angle

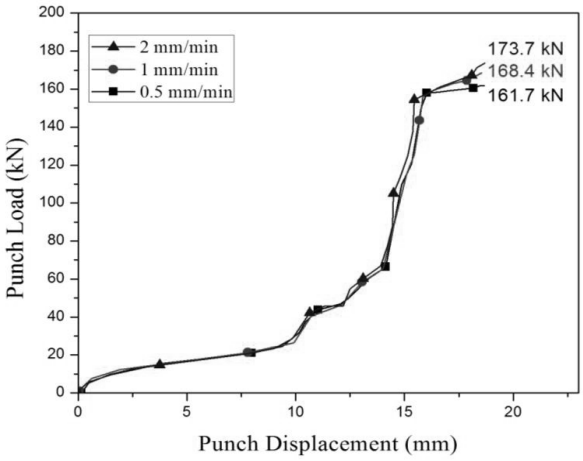

Figure 4.3 Variation of punch load with punch travel at friction factor of 0.18 at 45° Die angle

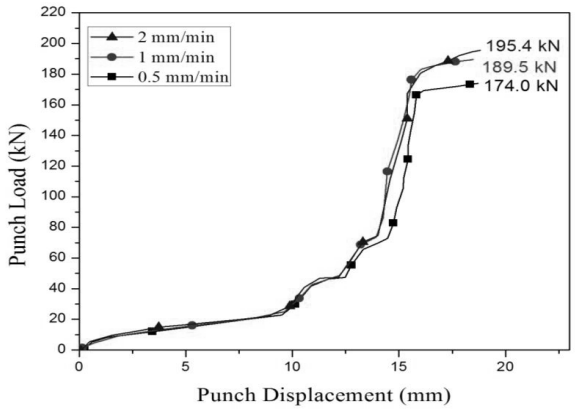

Figure 4.4 Variation of punch load with punch travel at friction factor of 0.37 at 45° Die angle

In the figures 4.2 to 4.4 gives comparison of punch load with punch movement for different velocities using lubricant MoS2 + grease (60:40) with friction factor 0.12,0.18,0.37 and Die angle 45° and 100% grease and no lubrication respectively. The maximum extrusion loads at flashing are provided in Table 4.1. It is evident from the Table 4.1 that with increase of friction the load increases and also with ram velocity load requirements increases because of work hardening.

4.2.2 Variation of punch load with punch travel at friction factor of 0.12, 0.18, 0.37 at 60° Die angle

Figures 4.5 to 4.7 gives comparison of punch load with punch movement for different velocities using lubricant MoS2 + grease (60:40) with friction factor 0.12,0.18,0.37 and Die angle 60° and 100% grease and no lubrication respectively. The maximum extrusion loads at flashing are provided in Table 4.2. The ram displacement behaviors show that the total process can be assumed to consist of four stages:

- Initial stage, the load gradually increases backward extrusion takes place,
- Second stage, forward and lateral extrusion takes place,
- Combined stage, both extrusion and forging takes place for corner filling,
- The unsteady state stage, steep rise in load to form flash. As the metal flow are hindered, redundant work increases, subsequently the load increases unsteadily.

Table No. 4.2 for 60° Die angle

Sr. No.	Friction factor	Ram velocity mm/min	Peak load at flashing, kN
1	0.12	0.5	150.2
2		1.0	153.21
3		2.0	160.8
4	0.18	0.5	152.7
5		1.0	166.2
6		2.0	174.5
7	0.37	0.5	177.0
8		1.0	185.6
9		2.0	193.4

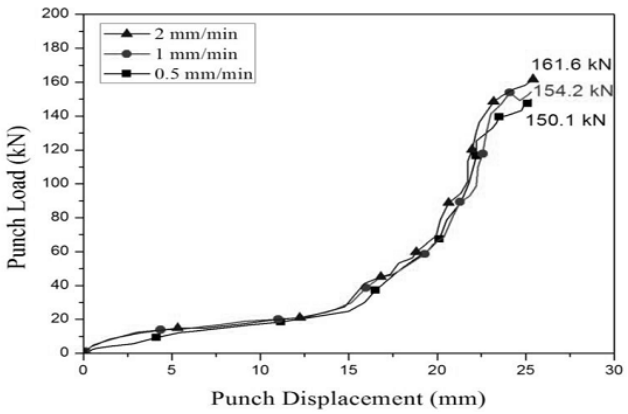

Figure 4.5 Variation of punch load with punch travel at friction factor of 0.12 at 60° Die angle

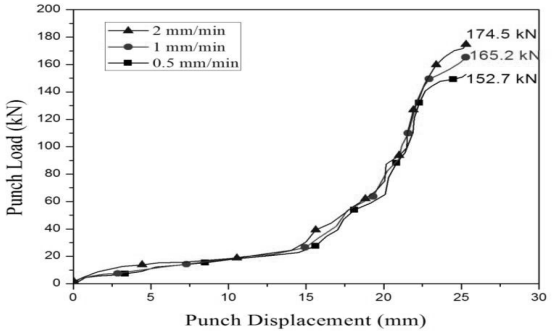

Figure 4.6 Variation of punch load with punch travel at friction factor of 0.18 at 60° Die angle

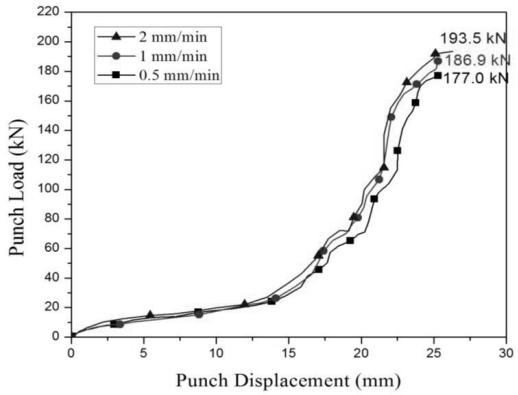

Figure 4.7 Variation of punch load with punch travel at friction factor of 0.37 at 60° Die angle

In the figures 4.5 to 4.7 gives comparison of punch load with punch movement for different velocities using lubricant MoS2 + grease (60:40) with friction factor 0.12,0.18,0.37 and Die angle 60° and 100% grease and no lubrication respectively. The maximum extrusion loads at flashing are provided in Table 4.2. It is evident from the Table 4.2 that with increase of friction the load increases and also with ram velocity load requirements increases because of work hardening.

4.2.3 Variation of punch load with punch travel at friction factor of 0.12, 0.18, 0.37 at 75° Die angle

Figures 4.8 to 4.10 gives comparison of punch load with punch movement for different velocities using lubricant MoS2 + grease (60:40) with friction factor 0.12,0.18,0.37 and Die angle 75° and 100% grease and no lubrication respectively. The maximum extrusion loads at flashing are provided in Table 4.3. The ram displacement behaviors show that the total process can be assumed to consist of four stages:

- Initial stage, the load gradually increases backward extrusion takes place,
- Second stage, forward and lateral extrusion takes place,
- Combined stage, both extrusion and forging takes place for corner filling,
- The unsteady state stage, steep rise in load to form flash. As the metal flow are hindered, redundant work increases, subsequently the load increases unsteadily.

Table No. 4.3 for 70° Die angle

Sr. No.	Friction factor	Ram velocity (mm/min)	Peak load at flashing, kN
1	0.12	0.5	143.6
2		1.0	146.2
3		2.0	153.7
4	0.18	0.5	142.3
5		1.0	155.2
6		2.0	156.6
7	0.37	0.5	151.2
8		1.0	163.8
9		2.0	178.4

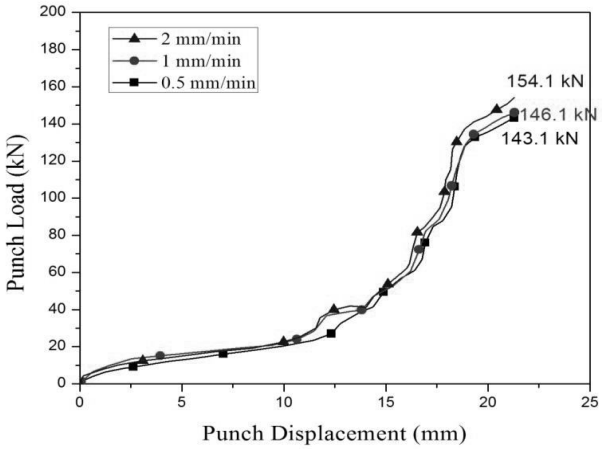

Figure 4.8 Variation of punch load with punch travel at friction factor of 0.12 at 75° Die angle

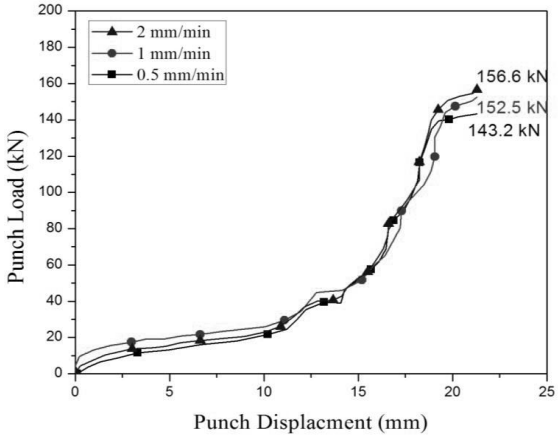

Figure 4.9 Variation of punch load with punch travel at friction factor of 0.18 at 70° Die angle

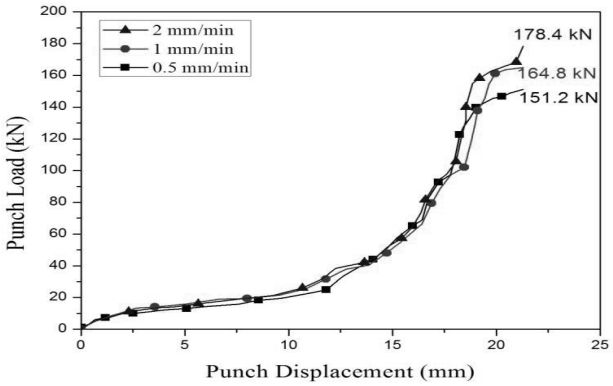

Figure 4.10 Variation of punch load with punch travel at friction factor of 0.37 at 70° Die angle

In the figures 4.8 to 4.10 gives comparison of punch load with punch movement for different velocities using lubricant MoS2 + grease (60:40) with friction factor 0.12,0.18,0.37 and Die angle 75° and 100% grease and no lubrication respectively. The maximum extrusion loads at flashing are provided in Table 4.3. It is evident from the Table 4.3 that with increase of friction the load increases and also with ram velocity load requirements increases because of work hardening.

4.3 Die Filling

In figure 4.11 shows the progressive change in shape of extrusion-forged product at different punch movements when the friction factor is 0.12 and the ram speed is 0.5 mm/min (as illustration). The die filling process substantiate that the total process can be thought of four stages as explained earlier, i.e., initial compression stage backward extrusion takes place during (0 - 10.0 mm of ram movement), in second stage during (10.0 - 16.0 mm ram) travel lateral extrusion takes place to form collar, during third stage (16.0 - 18.0 mm ram travel) corner filling and forward extrusion takes place, and in last stage (18.0 -18.3 mm ram travel) flash is formed to complete the process. It also explains that combined extrusion forging processes takes place simultaneously till the die cavity is completely filled, after which flash is started to form.

Metal flow pattern show the contour of displacements in both the horizontal and axial direction after 10.0 mm, 16.0 mm, 18.0 mm and 18.3 mm ram displacements respectively at 0.5 mm/min ram velocity with constant frictional conditions. Similarly, Figures above shows the contour of displacements in both the horizontal and axial direction after 10.0 mm, 16.0 mm, 18.0 mm and 18.3 mm ram displacements respectively with varying ram velocities at 0.13 frictional condition. The degree of distortion of gridlines at different stages confirms the load ram displacement behavior. Severe grid distortion at flashing stage validates the maximum load due to maximum redundant work. It is also seen that the whole billet, rather than part close to punch, is deforming simultaneously in different directions. Also, there is a non-uniform grid distortion due to friction at die-billet interface.

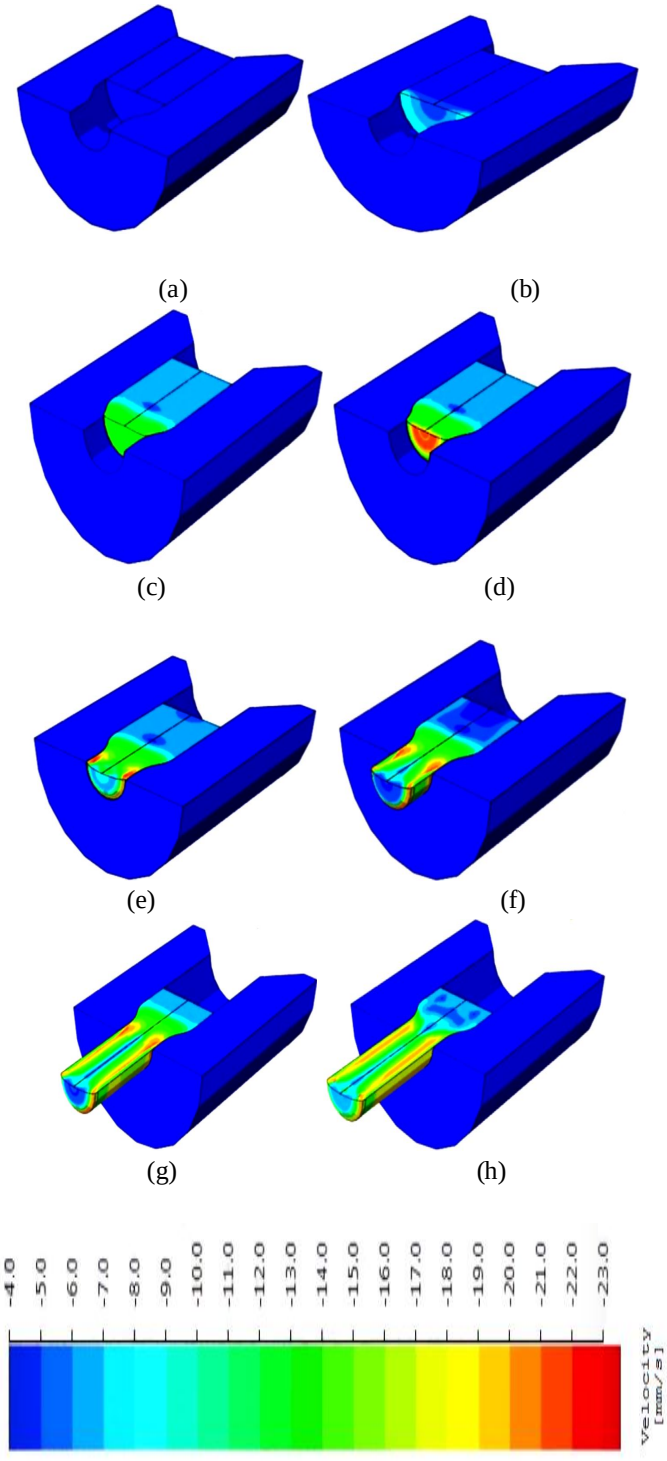

Figure 4.11 Different frame by frame images of a billetes coming out from the cavity with die angle 45 degree.

4.4 Validation FEM model

The simulation had also performed for different die angles and stress strain curve as shown figure 4.12 which is obtain from ANSYS.

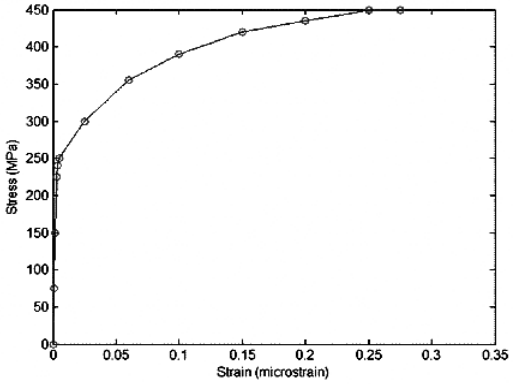

Figure 4.12 stress strain for Billet

The table 4.4 and 4.5 shows the comparison of experimental and FEM simulated results

Table No. 4.4 Experimental and FEM Simulated Results

Extrusion Angle	Experimental Tensile strength (N/mm²)	Simulated Tensile strength (N/mm²)	Percentage Error (%)
45	1082	1070.12	1.11
60	1068	1059.78	0.75
75	1062	1059.01	0.28

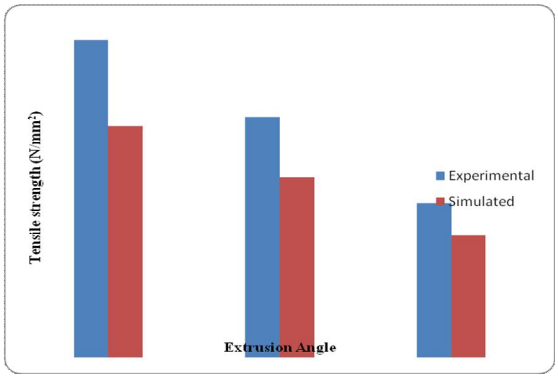

Figure 4.13 Comparison between Experimental and Simulated Results at Graph of Tensile Strength (N/mm^2)

Table No. 4.5 Experimental and FEM Simulated Results

Extrusion Angle	Experimental Yield strength (N/mm²)	Simulated Yield strength (N/mm²)	Percentage Error
45	968	959.01	0.92
60	960	953.70	0.66
75	951	947.59	0.36

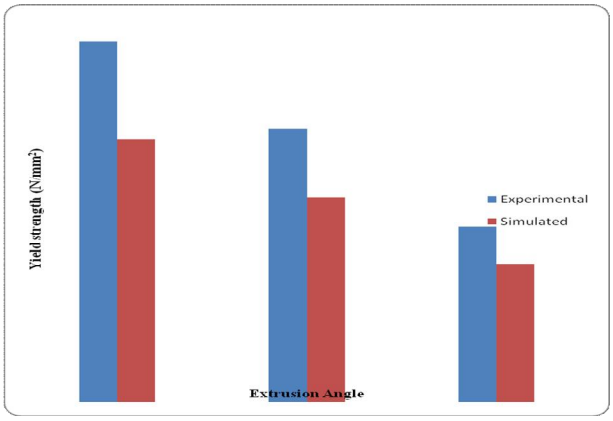

Figure 4.14 Comparison between Experimental and Simulated Results at Graph of Yield Strength (N/mm^2)

The results obtained can be summarized as in the present chapter the finite element analysis for three different types of dies were performed by simulation processes. Similar conditions of experimental analysis are taken into account for performing the present FEM analysis. Combination of three types of dies with frictional conditions. Different stages of deformation for 45 degree dies are performed for clear understating of die filling. Different stages of die filling data are used for further comparison analysis. Different stages of metal flow pattern for 45 degree dies are obtained for clear understanding of grain flow and shear effected regions. Shows the punch load and punch displacement variation.

V. CONCLUSION

Simulations were carried out for the analysis of the Ti6Al4V composite were successfully indirect different extrusion angles of die in FEM processed (45°, 60° and75°).

- Initial compression stage, in which the load gradually increases, forms a small indentation hole by backward extrusion.
- Second stage, in which radial extrusion formation of billets are formed along with the forward extrusion of

the part was performed, combined stage, corner die filling and extrusion of part was done,

- The unsteady state stage, in which there is a steep rise in load. In this stage, flash is formed, as the metal flow has hindered and controlled, the load increases unsteadily.

In case of third product metal flows out through the exit extrusion die present at the bottom, hence no flash provision is equipped.

The last product is manufactured by multi stage extrusion process in which the first product is the initial input specimen. Hence, the process is thought consists of two stages.

The results obtained can be summarized as below:

- In the present chapter the finite element analysis for three different types of dies were performed by simulation processes.
- Similar conditions of experimental analysis are taken into account for performing the present FEM analysis. Combination of three types of dies with frictional conditions
- Different stages of deformation for 45 degree dies are performed for clear understating of die filling. Different stages of die filling data are used for further comparison analysis.
- Different stages of metal flow pattern for 45 degree dies are obtained for clear understanding of grain flow and shear effected regions.
- Shows the punch load and punch displacement variation

5.2 Future Scope

New methodologies, such as computer simulations using the morphologies from real microstructures, and micro indentation to determine the constitutive properties of (TiB+TiC) Ti6Al4V phases, are allowing for more accurate predictions of material properties. Overall, (TiB+TiC) Ti6Al4V materials have shown promise for these state of the art materials design methodologies.

For further analysis we can do simulation at indirect different extrusion angles of die in FEM process and see the result in term of load and punch load variation. Also analysis the different sort of stages of extrusion process for metal composite material as also mix the material in different proportion and see results in term of what effect on their tensile strength and shear stress.

REFERENCES

[1] Mohamed A. Taha, “Practicalization of cast metal matrix composites (MMCCs)”, Materials and Design, 22 (2001), 431-441.
[2] BekirSadıkUnlu, “Investigation of tribological and mechanical properties Al2O3–SiC reinforced Al composites manufactured by casting or P/M method”, Materials and Design, 29 (2008), 2002–2008.
[3] AhmetHascalik and NuriOrhan, “Effect of particle size on the friction welding of Al2O3 reinforced 6061Al alloy composite and SAE 1020 steel”, Materials and Design, 28 (2007), 313–317.
[4] FevziBedir, “Characteristic properties of Al–Cu–SiCp and Al–Cu–B4Cp composites produced by hot pressing method under nitrogen atmosphere”, Materials and Design, 28 (2007), 1238–1244.
[5] HalilArik, “Effect of mechanical alloying process on mechanical properties of a-Si3N4 reinforced aluminum-based composite materials”, Materials and Design, 29 (2008), 1856–1861.
[6] Hideki Sekine and RongChent, “A combined microstructure strengthening analysis of SiCp/Al metal matrix composites”, Composites, 26 (1995) 183- 188.
[7] RecepEkici, M. Kemal Apalak , Mustafa Yıldırım , Fehmi Nair, “Effects of random particle dispersion and size on the indentation behavior of SiC particle reinforced metal matrix composites”, Materials and Design, 31 (2010) , 2818–2833.
[8] D.K. Dwivedi, “Adhesive wear behaviour of cast Aluminum–silicon alloys: Overview”, Materials and Design, 31 (2010), 2517–2531.
[9] MadevaNagaral, V Auradi, S. A. Kori, “Dry sliding wear behavior of graphite particulate reinforced Al6061 alloy composite materials”, Applied Mechanics and Materials, 592-594 (2014), 170-174.